

In Vivo Fluorescence Microscopy: Lessons From Observing Cell Behavior in Their Native Environment

Myunghwan Choi,^{1*}
Sheldon J. J. Kwok,^{1,2*}
and Seok Hyun Yun^{1,2}

¹Harvard Medical School and Wellman Center for Photomedicine, Massachusetts General Hospital, Boston, Massachusetts; and ²Harvard-MIT Health Sciences and Technology, Cambridge, Massachusetts
syun@hms.harvard.edu

*M. Choi and S. J. J. Kwok contributed equally to this work.

Microscopic imaging techniques to visualize cellular behaviors in their natural environment play a pivotal role in biomedical research. Here, we review how recent technical advances in intravital microscopy have enabled unprecedented access to cellular physiology in various organs of mice in normal and diseased states.

A central theme of physiology is to understand cellular function in the context of living systems. This has been traditionally achieved by histological examinations of cells in tissue or biochemical assays of cells in culture (20, 86, 115, 117). Although these methods can provide critical information, such as spatial associations of cells and molecular expressions, an ideal approach would allow us to study cells in vivo in real time as they interact with their natural environment. Recent advances in optical microscopy have made such an approach possible by enabling the visualization of individual cells in live animals. With the development of various chemical and genetic labeling techniques, intravital fluorescence microscopy has become a powerful tool in cell physiology.

Intravital microscopy provides several compelling advantages for the study of cell physiology. Most importantly, it offers a way to study live cellular events, such as proliferation, migration, differentiation, or intracellular ionic activity (3, 21, 86). Ex vivo model systems cannot fully recapitulate the multicellular microarchitecture, chemokine gradients, blood perfusion, and biomechanical forces. These limitations sometimes produce artifacts and mislead our interpretation. For example, a study based on a brain slice culture showed that the activation of astrocytic endfeet enwrapping the penetrating artery induced arterial constriction (80). However, a similar experiment with live mice led to the opposite finding that astrocyte activation predominantly leads to vasodilation (107). This discrepancy was later reconciled by the artifactual metabolic status introduced during brain slice preparation (38). Another advantage is that the use of a living animal allows follow-up of physiological changes over days in the same experimental subject. This is particularly useful in studying biological phenomena involving long-term kinetics, such as in development, stem cell physiology, and pathogenesis. It also enables the study of inter-individual variability, which is prevalent in biological phenomena.

Here, we review how intravital microscopy has been applied to study cellular physiology in various organs and organ systems in normal or diseased states (FIGURE 1). We focus on studies in mice, one of the most widely used animal models in biomedical research due to their genetic similarities to humans, short generation times, and established genetic lines. We will cover most major organ systems, including nervous, gastrointestinal, renal, respiratory, cardiovascular, musculoskeletal, hematological, reproductive, and endocrine systems. In each section, we will summarize technical developments toward attaining microscopic access to the tissue of interest, as well as their applications in studying cellular physiology in their native environment.

General Technical Considerations

Fluorescence is widely used in optical imaging due to its high efficiency and specificity along with a toolbox of various chemical and genetic probes to label molecules or cells of interest. Although exogenous chemical probes often provide higher quantum yield with simple and versatile labeling procedures, transgenic labeling by fluorescent proteins is becoming increasingly popular because of cell- or tissue-type specificity and constitutive replenishing of fluorophores enabling long-term tracing (35, 86).

The two most established modalities for intravital imaging are confocal fluorescence microscopy and two-photon microscopy. Confocal microscopy uses a pinhole to achieve optical sectioning in tissue with axial resolution of a few micrometers. Two-photon microscopy provides deeper access into biological tissues with depth of over hundreds of micrometers owing to its near-infrared wavelength having less scattering and absorption, and negligible out-of-focus signal due to nonlinear excitation (119). Light sheet microscopy has been rapidly adopted in the study of small animals such as the drosophila and mouse embryo where the

tissue is relatively thin, but it has not been widely used for adult mice and larger animals (108).

For successful application of intravital microscopy, it is important to understand anatomical constraints and choose an appropriate technical solution that allows observation of the tissue of interest with minimal perturbations. Most tissues other than the skin surface require particular preparation for obtaining optical access. For example, a skin-flap model is effective for reaching the lower dermis and subcutaneous tissue (FIGURE 2A). Some organs may be accessed by surgically removing the skin layers directly above the tissue of interest, but this approach may introduce the risk of compromising cellular physiology due to invasiveness. More importantly, irreversible surgical intervention prevents longitudinal observation over days. Optical window models have been developed to address this problem. Surgically installed, transparent glass windows permit chronic microscopic access to various organs, such as the dorsal skin, brain, and abdominal organs (FIGURES 2B AND 3). Another approach is to miniaturize the optical system by introducing micro-endoscopic probes (FIGURES 2C AND 4). Although the small-diameter probes often have lower resolution and smaller field of view compared with standard objective lenses, this approach allows minimally invasive access to internal tissues through natural orifices (e.g., colon, esophagus, trachea) or via small surgical openings that can be closed after imaging.

Another important technical challenge comes from the physiological motion of animals mainly due to breathing and heart beating. The motion introduces blurring artifacts during imaging, compromising spatial information. Although multiple approaches, such as time-gating (110) and adaptive motion tracking (65), have been proposed, the current gold-standard solution is to fix the tissue onto rigid fixatives by suture (47), glue (91), or suction pressure (50). The fixatives need to be specifically designed for each organ to ensure sufficient motion stabilization while minimizing interference with normal cellular physiology.

Applications to Physiology Systems

The Nervous System

Brain. Intravital imaging of the brain cortex has become the gold-standard technique in neuroscience to study the spatiotemporal activity of neuronal networks. There are several excellent review papers on brain imaging (53, 78). Several techniques to access the cortex exist: the open skull window, which is widely used but immunoreactivity is relatively high (44); the thinned skull window, which introduces less immunoreactivity but skull regrowth; and the reinforced thinned skull win-

dow, a newer technique that facilitates chronic imaging over months without need of immunosuppression (25). Kienast et al. studied the early phase dynamics of hematogenous metastasis into the brain from a single metastatic cell to macrometastasis (55). They measured important checkpoints toward macrometastasis, such as arrest at vascular branching points, extravasation, and persistent contact to microvessels. Shih et al. studied microvascular injury (99) induced by femtosecond blood occlusion (81) to show that the occlusion of single penetrating artery is sufficient to lead to cognitive deficits (FIGURE 3B). Long-term subcortical access has also been demonstrated by invasive endoscopy. Levene et al. implanted a microprism to image entire cortical columns (4). Baretto et al. implanted glass tubes to allow endoscopic access to the hippocampus (7) and measured neuronal activities encoding place cognition in behaving mice over weeks (120). By monitoring thousands of hippocampal place cells over weeks, Ziv et al. (120) found that retention of spatial information was highly dynamic day-to-day, with only 15–25% probability that an individual cell will recur in the same place code each day. Imaging of deeper subcortical regions, such as the thalamus, has been demonstrated by using 350- μ m-diameter side-view endoscopes (57, 58) (FIGURE 4A). Recently, Horton et al. demonstrated that three-photon microscopy at a spectral excitation window of 1,700 nm enables access to subcortical structures, such as hippocampus, within an intact mouse brain (45).

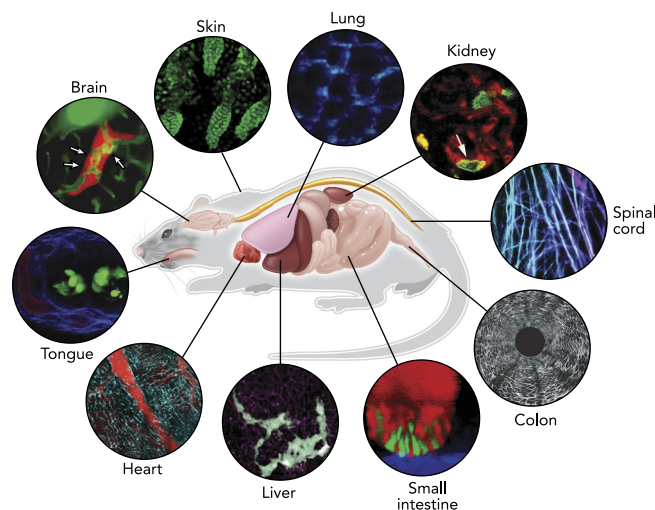


FIGURE 1. In vivo imaging in the mouse

Advances in optical techniques in conjunction with sample preparation methods allow microscopic visualization of cellular dynamics in various organs in a living experimental animal. Representative images in each organ acquired by intravital microscopy on mouse models are shown. Images reproduced with permission from Refs. 55 (brain), 92 (ear skin), 75 (lung), 23 (kidney), 29 (spinal cord), 61 (colon), 89 (small intestine), 90 (liver), 50 (heart), and unpublished observations of Choi M, Lee WM, Yun SH (tongue).

Spinal cord. Intravital microscopy has been used to study the dynamics of spinal cord injury and regeneration (111). Kerschensteiner et al. surgically exposed the spinal cord by laminectomy to monitor individual fluorescent axons in the spinal cords of living transgenic mice over several days after spinal injury (54). Importantly, they observed that many axons attempt regeneration within a day after injury but fail due to the inability of axons to grow back along its original trajectory. Later, Farrar et al. developed a chronic implanted window model and investigated the regeneration dynamics of a single disseminated axon over months (29, 113) (FIGURE 3C).

Eye. Confocal ophthalmoscopy has long been used in the study of the retina (97). In conjunction with adaptive optics, Geng et al. gained subcellular resolution to visualize retinal microstructures such as optic nerves, capillaries, and ganglion cells over a month (32). The cornea can be readily visualized by confocal fluorescence microscopy or second harmonic generation microscopy to study collagen structure (67, 114). Second harmonic generation microscopy is typically performed concurrently with two-photon fluorescence imaging since they can share the same femtosecond pulsed laser source (98).

Cochlea. Monfared et al. used a graded-index lens probe to visualize flowing red blood cells in several cochlear structures, including the round window membrane, spiral ligament, osseous spiral lamina, and basilar membrane (79).

Tongue. Choi et al. recently developed a tongue imaging window and used two-photon microscopy to measure the vascular perfusion in taste buds and physiological activation of the taste receptor cells in response to tastants administered either topically or intravenously (unpublished observations) (FIGURE 3E).

The Gastrointestinal System

Liver. Ritsma et al. developed an abdominal imaging window to track the growth of an individual colorectal cancer cell in the mouse liver to the formation of a micrometastasis (90) (FIGURE 3D). Time-lapse imaging over 10 h revealed significant cellular migration within pre-micrometastases but not within micro- or macrometastases. Subsequent pharmacological inhibition of cell migration significantly reduced the metastatic burden, suggesting migration inhibition as a valid target for cancer therapy. The abdominal imaging window also extended long-term capabilities to other organs, including the stomach, spleen, kidney, and pancreas (90, 91).

Small intestine. Ritsma et al. used an abdominal imaging window to study homeostasis of stem cells marked by *Lgr5* in the murine intestine (89) and identified a central region (crypt base) and border region (upper part of niche) in the intestinal stem-cell niche (FIGURE 3D). The central stem cells are biased toward survival compared with the border stem cells, which are biased toward loss and replacement. Interestingly, this dependence of self-renewal potential on stem cell position within the niche is consistent with the finding in a recent intravital microscopy study of the mouse hair follicle (93).

Colon. Side-view endomicroscopy has been used for longitudinal imaging of tumor-associated angiogenesis in a spontaneous colorectal cancer model (61) (FIGURE 4D). By coupling high-intensity femtosecond pulses to the probe, epithelium in the descending colon can be precisely ablated (18). Tracking epithelial regeneration in conjunction with genetic perturbation enabled the study of the *Card9* gene in epithelial restitution during the inflammatory response (102).

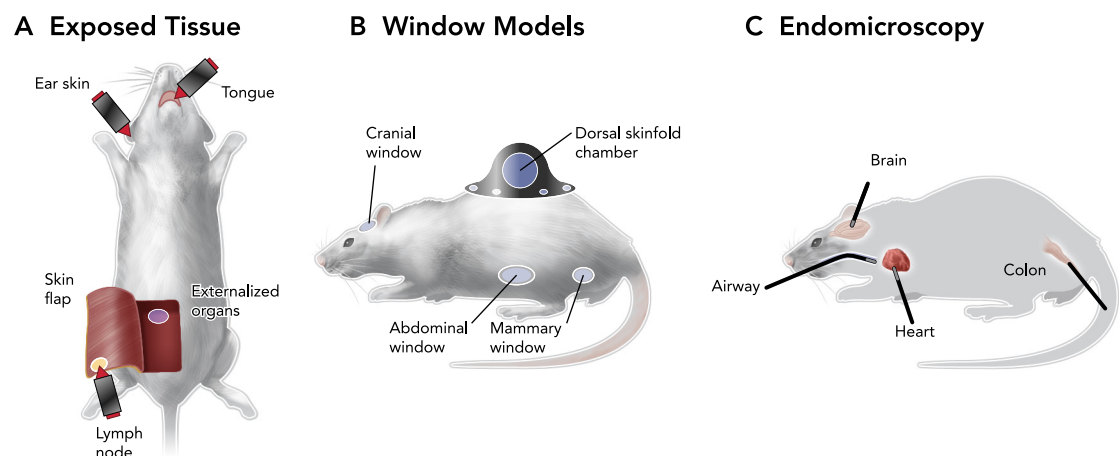


FIGURE 2. Ways to obtain microscopic access to various organs in vivo
 Three strategies for intravital imaging have been proposed to overcome limited penetration of light into tissue: through intact or surgically exposed tissue (A), by implanting an optically transparent window (B), or by inserting miniature endoscopic probes (C).

Esophagus. Kim et al. has demonstrated imaging of vascular structure of the esophagus by side-view endomicroscopy through the oral cavity (61). This should be useful to study pathogenesis of esophageal diseases, such as Barrett’s esophagus and esophageal malignancy.

The Renal System

Kidney. Laparoscopic access to abdominal organ has been particularly successful with the kidney (85). Two-photon imaging of the kidney has enabled quantification of glomerular filtration rate (51), fluid flow in the juxtglomerular interstitium (94), and renal albumin filtration (96). More recently, serial two-photon imaging was used to track single podocyte migration into the parietal Bowman’s capsule after unilateral ureteral ligation (41). These results challenge the classical view that podocytes are stationary. Another study looked at leukocyte recruitment in the glomerular microvasculature (23). It was found that acute glomerular inflammation increased the duration of leukocyte retention but not the total number of leukocytes recruited. These findings support the existence of a novel form of intravascular immune patrolling in the glomerulus and illustrate the advantage of intravital imaging in recording live biological processes. In histological analyses, neutrophils are rarely observed in healthy glomeruli, whereas increased numbers of neutrophils are observed in inflamed glomeruli. These data can be reconciled by the fact that histology provides a snapshot view

of the glomerulus at one particular time point; thus dynamic information, such as leukocyte dwell time, is lost. Fan et al. utilized endomicroscopy for minimally invasive serial tracking of immune cells over 2 wk (FIGURE 4B) (28).

Bladder and ureter. Using a front-view endomicroscope after laparotomy, Kim et al. demonstrated in vivo imaging of blood vessels and immune cells in the bladder and ureter (59). The urethral lumen may be accessible by introducing side-viewing endomicroscopy through its orifice.

The Cardiovascular and Respiratory Systems

Heart. Leukocyte trafficking has been studied within heterotopically transplanted hearts by partially exteriorizing the heart and gluing the surface to a glass coverslip (72). Li et al. examined the roles of endothelial adhesion proteins (Mac-1 and LFA-1) in neutrophil adhesion during ischemia reperfusion injury. Recently, a method of imaging the beating mouse heart in vivo was developed by combination of a motion stabilizer and real-time gating of particular phases in the respiratory and cardiac cycles (68). Serial intravital imaging over days was also demonstrated using endomicroscopy by inserting an endoscopic probe through the intercostal space while providing motion stabilization through a suction channel (50) (FIGURE 4C). Using this technique, Jung et al. observed patrolling monocytes rolling along vessel walls in the heart in the steady state and studied monocyte

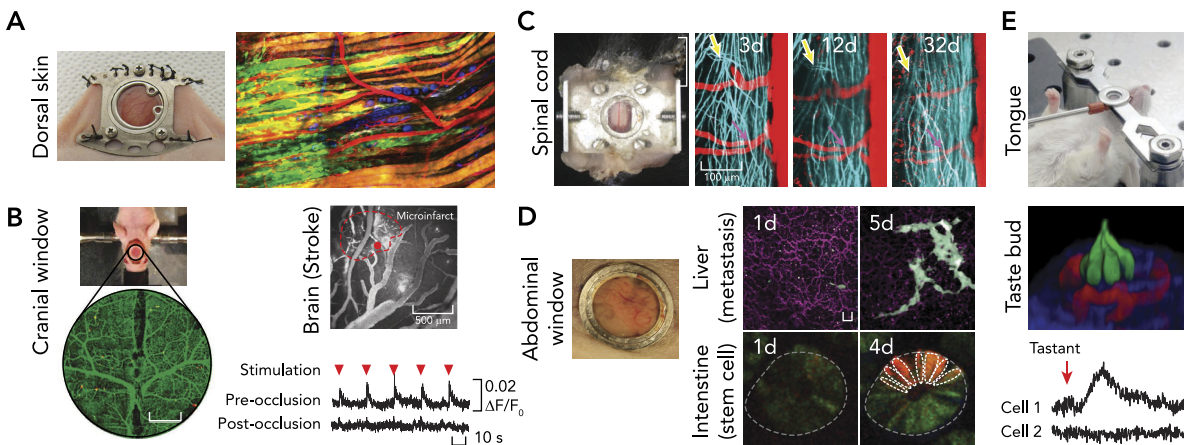


FIGURE 3. Imaging through optical windows
 A: dorsal skin. The photograph at left shows a dorsal skinfold chamber implanted on a nude mouse. The fluorescence image at right shows collective invasion of melanoma cells taken by multi-photon microscopy in the dorsal skinfold chamber. Images were reproduced from Ref. 74a with permission. B: brain. The photograph shows cranial window model implanted on a nude mouse after craniotomy. Change in neuronal responsiveness to limb stimulation (red arrowhead) after laser-induced microinfarct. Images reproduced from Ref. 99 with permission. C: spinal cord. The photograph at left shows imaging chamber implanted for chronic imaging of the spinal cord. Regeneration dynamics of the spinal axons (blue) at the injured area (yellow arrow) was traced over a month. Images reproduced from Ref. 29 with permission. D: abdominal organs. Glass window implanted on the abdomen (left) enabled tracking of cellular dynamics in various abdominal organs over time, such as cancer metastasis in the liver (top) and stem cell dynamics in small intestine (bottom). Scale bar, 20 μm. Images reproduced from Refs. 89–91 with permission. E: tongue. Top: preparation for imaging the mouse tongue. The fluorescence image (middle) shows a three-dimensional view of a taste bud (red, blood vessel; green, taste receptor cells). Bottom: intracellular calcium activity measured in the taste receptor cells after introducing artificial sweetener intravenously. Images reproduced with permission from unpublished observations of Choi M, Lee WM, Yun SH.

Downloaded from on January 5, 2015

recruitment after acute myocardial infarction. With the onset of the ischemic insult, monocytes are rapidly recruited first from the vascular reservoir and then from the spleen. The early infiltrating monocytes may subsequently recruit neutrophils in reperfusion injury as described in the lung (63).

Lung. For imaging cells in the lung, it is critical to immobilize the tissue by suction (75, 87), sutures, or glue to a transparent cover (42, 63, 106). Temporally gating in synchrony with natural or ventilated breathing further helps minimize movement artifacts. Kreisel et al. studied neutrophil extravasation during transplant-mediated ischemia reperfusion injury (63). They found that neutrophil clusters were associated with at least one monocyte, and depletion of monocytes dramatically reduced neutrophil extravasation. These observations suggest that monocytes mediate transendothelial migration of neutrophils, perhaps through local production of chemokine signals. Other studies have looked at the augmentation of alloimmunity by dendritic cell-neutrophil interactions after lung transplantation (64), neutrophil recruitment by platelet-derived chemokine heteromers in acute lung injury (39), and coordination of the immune response to pulmonary anthrax by macrophage-dendritic cell interactions (30).

Trachea. Kim et al. demonstrated imaging of tracheal epithelial cells through a side-view endoscope with a ventilation channel to facilitate physiological breathing during the imaging session (60) (FIGURE 4E). They performed endotracheal fluorescence imaging in live transgenic reporter mice to monitor the regeneration of Clara cells over 18 days after sulfur dioxide injury.

Musculoskeletal, Connective Tissue, and Skin

Muscle. Intravital microscopy has been applied to study different types of muscles. Under the mouse skin, there is a thin skeletal muscle layer, called the panniculus carnosus, which is not found in humans. By using a dorsal skinfold chamber, this skeletal muscle layer is readily accessible over time for studies of muscle contractility and associated blood perfusion as well as an orthotropic model of fibrosarcoma (FIGURE 3A). Smooth muscles in arteries or gastrointestinal organs are also accessible by appropriate chamber techniques. In particular, the control of arterial tone in the brain has been of primary interest due to its tight functional association with neuronal activity (16). Muscles have high autofluorescence and second-harmonic signals, providing imaging contrast without exogenous labeling. These intrinsic optical contrasts were used in conjunction with a miniature endoscopic probe to study the fate of orthotopically transplanted aorta in mice (2). Llewellyn et al. also used endomicroscopy to study the behavior of skeletal muscle in mice and humans (74). They were able to observe the dynamics of sarcomere contraction at millisecond-scale resolution. This method may be applied to study how sarcomere structure and lengths are altered with physical conditioning and in neuromuscular diseases.

Skeletal system. Bones and joints are of great interest for researchers studying autoimmune-related disorders (e.g., rheumatoid arthritis) or regenerative medicine to understand its maintenance and restitution. Williams et al. used time-series multiphoton microscopy to image molecular transport through the perichondrium in live juvenile mice

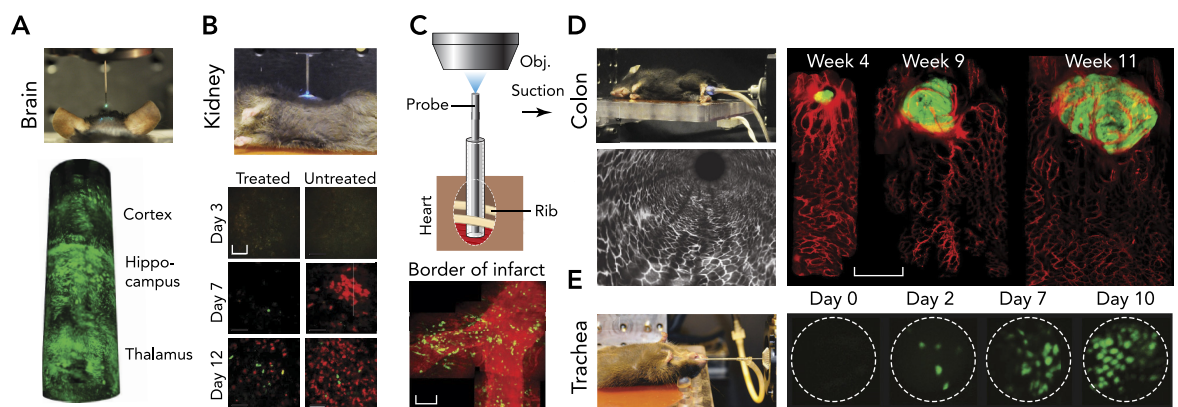


FIGURE 4. Endomicroscopy

A: brain. A side-viewing probe is inserted down to thalamus to visualize neurons labeled by fluorescent protein. Images reproduced from Ref. 57 with permission. B: kidney. Tracking of immune cells over 2 wk was shown with endomicroscopy of the kidney after minimal laparotomy. Scale bar, 50 μ m. Image reproduced from Ref. 28 with permission. C: heart. Endomicroscopy with a suction stabilizer was inserted through the intercostal space to access heart with minimal invasiveness for serial imaging over a day. Scale bar, 50 μ m. Images reproduced from Ref. 50 with permission. D: colon. Endomicroscopy for the colon. Tumorigenesis and angiogenesis were traced with dual-color endomicroscopic imaging in the descending colon. Scale bar, 500 μ m. Images reproduced from Ref. 59 with permission. E: trachea. Endomicroscope inserted through the trachea showed regeneration dynamics of epithelial cells after injury. Scale bar, 20 μ m. Images reproduced from Ref. 58 with permission.

(112). Minimally invasive access to the joint space might be feasible by direct insertion of an endoscopic probe (73).

Skin. As the external surface of mammals, skin is the most accessible tissue (FIGURE 2A). The skin has served as an excellent model to study tissue maintenance due to its continuous turnover and well defined stem cell niche (92). Rompolas et al. traced cell division and migration at the hair follicle and found that stem cell fate, i.e., whether stem cells remained uncommitted, generated precursors, or committed to a differentiated state, depended directly on the position of the stem cell within the follicle (93). The ear skin is also suitable for studying the dynamics of immune responses. Celli et al. investigated the dynamic response of donor and host cells during skin transplant (13, 71). Access to the subcutaneous side of the dorsal skin is achieved by surgical exposure. Miller et al. used the skin-flap model to study immune cell dynamics in lymph nodes (77). Numerous studies have employed the dorsal skinfold chamber for studies of tumorigenesis and measurements of physiological parameters such as hypoxia, interstitial pressure, and molecular diffusivity (5, 40, 47, 70, 88) (FIGURE 3A).

Adipose tissue. Intravital microscopy has been used to observe the vascular circulation, structure, and metabolic activity of interscapular brown adipose tissue (9). Imaging following short-term cold exposure showed rapid uptake of triglyceride-rich lipoproteins in brown adipose tissue.

Hematology and Immunology

Blood. Intravital microscopy has enabled the quantification of the number and flow characteristics of fluorescently labeled circulating cells (82), including rare circulating tumor cells (43) and immune cells (27). Because circulating cells are visualized in real time, their behavior, such as flowing, rolling, crawling, and extravasation, can be easily observed (50). Photoconvertible fluorophores have facilitated the study of dynamic cellular processes such as division, differentiation, and migration at single-cell resolution (12, 26). Using photoconversion, Dutta et al. showed that bone marrow cells relocate to the spleen following myocardial infarction (26).

Blood vessel. Vascular perfusion is a hallmark of living systems. Various physiological parameters, such as flow speed, direction, and oxygen saturation levels, can be measured by intravital microscopy (103). Several computational algorithms have been developed to extract blood flow velocities from data obtained through line-scanned imaging (24, 62). By tracing fluorescent nanoparticles, the spatial distributions of nanoparticles within blood vessels have been determined in agreement with

computer simulation (69). Intravital microscopy is a standard technique to study the structure and function (e.g., leakiness) of blood vasculature in the context of angiogenesis and anti-angiogenesis therapy. Furthermore, image-guided vascular occlusion, either by photodynamic effects or by using femtosecond laser irradiation has been used to disrupt microvessels in the cortex (100). Nishimura et al. demonstrated that a single blockage to a microvessel leads to local cortical ischemia (81).

Bone marrow. Due to its significant role in hematopoiesis, the bone marrow has been widely studied in the field of stem cell biology and immunology. The bone marrow in the skull (i.e., calvarium bone marrow) is easily accessible by exposing the scalp (101). Celso et al. studied the homing and early engraftment of transplanted hematopoietic stem and progenitor cells in the calvarium bone marrow (14). Using a similar technique, Fujisaki et al. found that the hematopoietic stem cell niche in the bone marrow is an immune-privileged site similar to those observed in the testis, hair follicle, and placenta (31), and resident regulatory T cells play a critical role for protecting allografted hematopoietic stem/progenitor cells. Spencer et al. measured the local oxygen concentration levels in the bone marrow by two-photon phosphorescence lifetime microscopy (103).

Spleen. Swirski et al. imaged an exteriorized spleen to observe an endogenous, undifferentiated reservoir of monocytes in the subcapsular red pulp of the spleen (105). The marginal zone, the interface between the red pulp and lymphoid white pulp of the spleen, has also been studied by a similar technique (6). Rapid marginal zone B-cell shuttling was observed, with at least 20% of marginal zone B cells exchanging between the marginal zone and follicle every hour. This data provides a mechanism for explaining how blood-borne antigens are rapidly delivered to splenic follicles.

Lymphatic system. Immune cell physiology in the lymph node has been extensively studied by using two-photon microscopy (33, 104). In one of the earliest studies, Mempel et al. looked at T-cell migration and interactions with dendritic cells at surgically exposed popliteal lymph nodes and revealed three successive stages of T-cell priming by dendritic cells: transient serial encounters with dendritic cells, stable contacts leading to cytokine production, and high motility and rapid proliferation (76).

The Reproductive System

Mammary glands. Kedrin et al. developed a mammary imaging window to track orthotopic breast tumors and observed that intravasation and infiltration of breast tumor cells were significantly enhanced in vascular microenvironments (52). A

later study showed that intravasation of breast carcinoma cells was significantly diminished by silencing the expression of neural Wiskott-Aldrich syndrome protein (36). Another study looked at the role of a regulator of actin polymerization and cell migration in breast tumor metastasis (95).

Ovary. Zhong et al. used endomicroscopic fluorescence imaging in tracking the progression and treatment of ovarian cancer (118). Using this technique, Choi et al. revealed the genetic origin (i.e., AIMP2 gene) of chemoresistance in ovarian cancer (15).

Prostate. Ghosh et al. used a fluorescent sensor for zinc along with confocal intravital microscopy to develop a novel imaging approach for detection of early stage prostate adenocarcinoma (34).

The Endocrine System

Pancreas. As the therapeutic target of diabetes, pancreatic islet cells are of particular interest to biomedical researchers. Through longitudinal imaging, Abdulreda et al. monitored immune responses following transplantation of pancreatic islets into the anterior chamber of the eye (1). Coppieters et al. visualized and analyzed the kinetics of killing islet cells mediated by cytotoxic T lymphocytes in a diabetic mouse model (22). Real-time imaging of blood flow in pancreatic islets has also been demonstrated (83).

Thyroid, parathyroid, and adrenal glands. To date, there has been no reported intravital microscopy study of the thyroid, parathyroid, and adrenal glands.

Ongoing Advances and Future Perspectives

In recent years, the development of various window models and endomicroscopy has extended the capabilities of intravital imaging beyond imaging superficial tissues and allowed longitudinal observation of cell physiology. Further technical advances to observe intact cellular behaviors with higher spatiotemporal resolution, deeper optical penetration, comprehensive volumetric views, and prolonged periods of time should have high impacts. Some of the promising approaches include super-resolution imaging, such as stimulated emission depletion (STED) microscopy, which has enabled the visualization of dendritic spine morphology in a living mouse brain (10). Advances in endomicroscopy are also actively pursued to achieve higher optical performance with better accessibility. High-resolution endomicroscopy was achieved by introducing a micro-lens and was demonstrated to resolve dendritic spines on hippocampal neurons (8). Optical beam shaping enabled wide-field imaging through thin, flexible

multimode fibers (19). There are also attempts to develop implantable optical systems using biocompatible or biodegradable optical materials (17, 84).

Beyond the mechanistic understanding of cell physiology in experimental animals, optical imaging has considerable potential to be used for humans in clinical settings. Fluorescence whole-body imaging systems in conjunction with tailored near-infrared fluorophores are under clinical trials for intraoperative image-guided surgeries (66, 109). Confocal laser endomicroscopes are commercially available and have been applied for detecting gastrointestinal abnormalities, such as Barrett's esophagus (11, 56) and colonic dysplasia (46), based on either clinically approved fluorescence dyes or label-free tissue scattering. Intrinsic nonlinear contrasts, such as second harmonic generation, two-photon autofluorescence, or stimulated Raman scattering (49), have a potential to be useful for providing histological-grade images for diagnosis or intraoperative tumor-margin detection. Elastic light scattering from tissues is also a useful imaging contrast. A tethered capsule endomicroscope system based on optical coherence tomography allowed less invasive imaging of the gastrointestinal tract with deeper penetration (37). Intravascular catheters using fluorescence combined with optical coherence tomography (48, 116) have been used for assessing plaques in coronary atherosclerosis.

Technological advances in intravital microscopy have enabled observation of cells in their native environments. Nearly all organs are now accessible by combining optical microscopy with endoscopic probes or implanted chamber techniques. With continuing progress in imaging instruments, as well as fluorescent probes and animal models, intravital fluorescence microscopy is expected to find increasing applications in the study of cellular physiology. ■

We thank Jiahe Zhang for help with the illustration of mouse schematics.

This work was funded in part by the U.S. National Institutes of Health (U54 CA-143837, P41 EB-015903), the U.S. National Science of Foundation (ECS-1101947), and a postdoctoral fellowship from the National Research Foundation of Korea (NRF-2013R1A6A3A03060958).

No conflicts of interest, financial or otherwise, are declared by the author(s).

Author contributions: M.C., S.J.K., and S.H.Y. prepared figures; M.C., S.J.K., and S.H.Y. drafted manuscript.

References

1. Abdulreda MH, Faleo G, Molano RD, Lopez-Cabezas M, Molina J, Tan Y, Echeverria OAR, Zahr-Akrawi E, Rodriguez-Diaz R, Edlund PK. High-resolution, noninvasive longitudinal live imaging of immune responses. *Proc Natl Acad Sci USA* 108: 12863–12868, 2011.

2. Akiyoshi T, Lee W, Chase C, Alessandrini A, Sebastian D, Della Pelle P, Connolly S, Farkash E, Yun SH, Russell P. In vivo two photon microscopy of aortic allografts: a new tool for investigation of the dynamics of graft vascular rejection. *Am J Transplant* 12: 466, 2012.
3. Alivisatos AP, Andrews AM, Boyden ES, Chun M, Church GM, Deisseroth K, Donoghue JP, Fraser SE, Lippincott-Schwartz J, Looger LL, Masmanidis S, McEuen PL, Nurmikko AV, Park H, Peterka DS, Reid C, Roukes ML, Scherer A, Schnitzer M, Sejnowski TJ, Shepard KL, Tsao D, Turrigiano G, Weiss PS, Xu C, Yuste R, Zhuang X. Nanotools for neuroscience and brain activity mapping. *ACS Nano* 7: 1850–1866, 2013.
4. Andermann ML, Gilfoy NB, Goldey GJ, Sachdev RN, Wölfel M, McCormick DA, Reid RC, Levene MJ. Chronic cellular imaging of entire cortical columns in awake mice using micropisms. *Neuron* 80: 900–913, 2013.
5. Ariotti S, Beltman JB, Chodaczek G, Hoekstra ME, van Beek AE, Gomez-Eerland R, Ritsma L, van Rheenen J, Marée AF, Zal T. Tissue-resident memory CD8⁺ T cells continuously patrol skin epithelia to quickly recognize local antigen. *Proc Natl Acad Sci USA* 109: 19739–19744, 2012.
6. Arnon TI, Horton RM, GrigoroVA IL, Cyster JG. Visualization of splenic marginal zone B-cell shuttling and follicular B-cell egress. *Nature* 493: 684–688, 2013.
7. Barretto RP, Ko TH, Jung JC, Wang TJ, Capps G, Waters AC, Ziv Y, Attardo A, Recht L, Schnitzer MJ. Time-lapse imaging of disease progression in deep brain areas using fluorescence microendoscopy. *Nat Med* 17: 223–228, 2011.
8. Barretto RP, Messerschmidt B, Schnitzer MJ. In vivo fluorescence imaging with high-resolution microlenses. *Nat Meth* 6: 511–512, 2009.
9. Bartelt A, Bruns OT, Reimer R, Hohenberg H, Ittrich H, Peldschus K, Kaul MG, Tromsdorf UI, Weller H, Waurisch C. Brown adipose tissue activity controls triglyceride clearance. *Nat Med* 17: 200–205, 2011.
10. Berning S, Willig KI, Steffens H, Dibaj P, Hell SW. Nanoscopy in a living mouse brain. *Science* 335: 551, 2012.
11. Bird-Lieberman EL, Neves Aa Lao-Sirieix P, O'Donovan M, Novelli M, Lovat LB, Eng WS, Mahal LK, Brindle KM, Fitzgerald RC. Molecular imaging using fluorescent lectins permits rapid endoscopic identification of dysplasia in Barrett's esophagus. *Nat Med* 18: 315–321, 2012.
12. Carlson AL, Fujisaki J, Wu J, Rannels JM, Turcotte R, Celso CL, Scadden DT, Strom TB, Lin CP. Tracking single cells in live animals using a photoconvertible near-infrared cell membrane label. *PLoS One* 8: e69257, 2013.
13. Celli S, Albert ML, Bousso P. Visualizing the innate and adaptive immune responses underlying allograft rejection by two-photon microscopy. *Nat Med* 17: 744–749, 2011.
14. Celso CL, Lin CP, Scadden DT. In vivo imaging of transplanted hematopoietic stem and progenitor cells in mouse calvarium bone marrow. *Nat Prot* 6: 1–14, 2011.
15. Choi JW, Lee JW, Kim JK, Jeon HK, Choi JJ, Kim DG, Kim BG, Nam DH, Kim HJ, Yun SH, Kim S. Splicing variant of AIMP2 as an effective target against chemoresistant ovarian cancer. *J Mol Cell Biol* 4: 164–173, 2012.
16. Choi M, Choi C, Yoon J. Label-free optical control of arterial contraction. *J Biomed Optics* 15: 015006-015006-015006, 2010.
17. Choi M, Choi JW, Kim S, Nizamoglu S, Hahn SK, Yun SH. Light-guiding hydrogels for cell-based sensing and optogenetic synthesis in vivo. *Nat Photonics* 7: 987–994, 2013.
18. Choi M, Yun SH. In vivo femtosecond endosurgery: an intestinal epithelial regeneration-after-injury model. *Optics Express* 21: 30842–30848, 2013.
19. Choi Y, Yoon C, Kim M, Yang TD, Fang-Yen C, Dasari RR, Lee KJ, Choi W. Scanner-free and wide-field endoscopic imaging by using a single multimode optical fiber. *Phys Rev Lett* 109: 203901, 2012.
20. Conchello JA, Lichtman JW. Optical sectioning microscopy. *Nat Meth* 2: 920–931, 2005.
21. Condeelis J, Segall JE. Intravital imaging of cell movement in tumours. *Nat Rev Cancer* 3: 921–930, 2003.
22. Coppieters K, Amirian N, von Herrath M. Intravital imaging of CTLs killing islet cells in diabetic mice. *J Clin Invest* 122: 119, 2012.
23. Devi S, Li A, Westhorpe CLV, Lo CY, Abeynaik LD, Snelgrove SL, Hall P, Ooi JD, Sobey CG, Kitching ar, Hickey MJ. Multiphoton imaging reveals a new leukocyte recruitment paradigm in the glomerulus. *Nat Med* 19: 107–112, 2013.
24. Drew PJ, Blinder P, Cauwenberghs G, Shih AY, Kleinfeld D. Rapid determination of particle velocity from space-time images using the Radon transform. *J Comp Neurol* 29: 5–11, 2010.
25. Drew PJ, Shih AY, Driscoll JD, Knutsen PM, Blinder P, Davalos D, Akassoglou K, Tsai PS, Kleinfeld D. Chronic optical access through a polished and reinforced thinned skull. *Nat Meth* 7: 981–984, 2010.
26. Dutta P, Courties G, Wei Y, Leuschner F, GorbatoV R, Robbins CS, Iwamoto Y, Thompson B, Carlson AL, Heidt T. Myocardial infarction accelerates atherosclerosis. *Nature* 487: 325–329, 2012.
27. Fan Z, Spencer JA, Lu Y, Pitsillides CM, Singh G, Kim P, Yun SH, Toxavidis V, Strom TB, Lin CP. In vivo tracking of 'color-coded' effector, natural and induced regulatory T cells in the allograft response. *Nat Med* 16: 718–722, 2010.
28. Fan Z, Spencer JA, Lu Y, Pitsillides CM, Singh G, Kim P, Yun SH, Toxavidis V, Strom TB, Lin CP, Koulmanda M. In vivo tracking of 'color-coded' effector, natural and induced regulatory T cells in the allograft response. *Nat Med* 16: 718–722, 2010.
29. Farrar MJ, Bernstein IM, Schlafer DH, Cleland TA, Fetcho JR, Schaffer CB. Chronic in vivo imaging in the mouse spinal cord using an implanted chamber. *Nat Meth* 9: 297–302, 2012.
30. Fiore D, Deman P, Trescos Y, Mayol JF, Mathieu J, Vial JC, Douady J, Tournier JN. Two-photon intravital imaging of lungs during anthrax infection reveals long-lasting macrophage-dendritic cell contacts. *Infect Immun* 82: 864–872, 2013.
31. Fujisaki J, Wu J, Carlson AL, Silberstein L, Putheti P, Larocca R, Gao W, Saito TI, Celso CL, Tsuyuzaki H. In vivo imaging of Treg cells providing immune privilege to the haematopoietic stem-cell niche. *Nature* 474: 216–219, 2011.
32. Geng Y, Dubra A, Yin L, Merigan WH, Sharma R, Libby RT, Williams DR. Adaptive optics retinal imaging in the living mouse eye. *Biomed Optics Express* 3: 715–734, 2012.
33. Germain RN, Robey EA, Cahalan MD. A decade of imaging cellular motility and interaction dynamics in the immune system. *Science* 336: 1676–1681, 2012.
34. Ghosh SK, Kim P, Zhang Xa Yun SH, Moore A, Lippard SJ, Medarova Z. A novel imaging approach for early detection of prostate cancer based on endogenous zinc sensing. *Cancer Res* 70: 6119–6127, 2010.
35. Giepmans BN, Adams SR, Ellisman MH, Tsien RY. The fluorescent toolbox for assessing protein location and function. *Science* 312: 217–224, 2006.
36. Gligorijevic B, Wyckoff J, Yamaguchi H, Wang Y, Roussos ET, Condeelis J. N-WASP-mediated invadopodium formation is involved in intravasation and lung metastasis of mammary tumors. *J Cell Sci* 125: 724–734, 2012.
37. Gora MJ, Sauk JS, Carruth RW, Gallagher Ka Suter MJ, Nishioka NS, Kava LE, Rosenberg M, Bouma BE, Tearney GJ. Tethered capsule endomicroscopy enables less invasive imaging of gastrointestinal tract microstructure. *Nat Med* 19: 238–240, 2013.
38. Gordon GR, Choi HB, Rungta RL, Ellis-Davies GC, MacVicar BA. Brain metabolism dictates the polarity of astrocyte control over arterioles. *Nature* 456: 745–749, 2008.
39. Grommes J, Alard JE, Drechsler M, Wantha S, Mörgelin M, Kuebler WM, Jacobs M, von Hundelshausen P, Markart P, Wygrecka M, Preissner KT, Hackeng TM, Koenen RR, Weber C, Soehnlein O. Disruption of platelet-derived chemokine heteromers prevents neutrophil extravasation in acute lung injury. *Am J Respir Crit Care Med* 185: 628–636, 2012.
40. Guba M, Von Breitenbuch P, Steinbauer M, Koehl G, Flegel S, Hornung M, Bruns CJ, Zuelke C, Farkas S, Anthuber M. Rapamycin inhibits primary and metastatic tumor growth by antiangiogenesis: involvement of vascular endothelial growth factor. *Nat Med* 8: 128–135, 2002.
41. Hackl MJ, Burford JL, Villanueva K, Lam L, Suszták K, Schermer B, Benzing T, Pesti-Peterdi J. Tracking the fate of glomerular epithelial cells in vivo using serial multiphoton imaging in new mouse models with fluorescent lineage tags. *Nat Med* 19: 1661–1666, 2013.
42. Hanna G, Fontanella A, Palmer G, Shan S, Radloff DR, Zhao Y, Irwin D, Hamilton K, Boico A, Piantadosi Ca Blueschke G, Dewhirst M, McMahon T, Schroeder T. Automated measurement of blood flow velocity and direction and hemoglobin oxygen saturation in the rat lung using intravital microscopy. *Am J Physiol Lung Cell Mol Physiol* 304: L86–L91, 2013.
43. He W, Wang H, Hartmann LC, Cheng JX, Low PS. In vivo quantitation of rare circulating tumor cells by multiphoton intravital flow cytometry. *Proc Natl Acad Sci USA* 104: 11760–11765, 2007.
44. Holtmaat A, Bonhoeffer T, Chow DK, Chuckoree J, De Paola V, Hofer SB, Hübener M, Keck T, Knott G, Lee WCA. Long-term, high-resolution imaging in the mouse neocortex through a chronic cranial window. *Nat Prot* 4: 1128–1144, 2009.
45. Horton NG, Wang K, Kobat D, Clark CG, Wise FW, Schaffer CB, Xu C. In vivo three-photon microscopy of subcortical structures within an intact mouse brain. *Nat Photonics* 7: 205–209, 2013.
46. Hsiung PL, Hardy J, Friedland S, Soetikno R, Du CB, Wu AP, Sahbaie P, Crawford JM, Lowe AW, Contag CH, Wang TD. Detection of colonic dysplasia in vivo using a targeted heptapeptide and confocal microendoscopy. *Nat Med* 14: 454–458, 2008.
47. Huang Q, Shan S, Braun RD, Lanzen J, Anyrhambatla G, Kong G, Borelli M, Corry P, Dewhirst MW, Li CY. Noninvasive visualization of tumors in rodent dorsal skin window chambers. *Nat Biotechnol* 17: 1033–1035, 1999.
48. Jaffer FA, Vinegoni C, John MC, Aikawa E, Gold HK, Finn AV, Ntzachristos V, Libby P, Weissleder R. Real-time catheter molecular sensing of inflammation in proteolytically active atherosclerosis. *Circulation* 118: 1802–1809, 2008.
49. Ji M, Orringer DA, Freudiger CW, Ramkissoon S, Liu X, Lau D, Golby AJ, Norton I, Hayashi M, Agar NY. Rapid, label-free detection of brain tumors with stimulated Raman scattering microscopy. *Sci Transl Med* 5: 201ra119, 2013.

50. Jung K, Kim P, Leuschner F, Gorbato R, Kim JK, Ueno T, Nahrendorf M, Yun SH. Endoscopic time-lapse imaging of immune cells in infarcted mouse hearts. *Circ Res* 112: 891–899, 2013.
51. Kang J, Toma I, Sipos A. Quantitative imaging of basic functions in renal (patho) physiology. *Am J Physiol Renal Physiol* 291: F495–F502, 2006.
52. Kedrin D, Gligorijevic B, Wyckoff J, Verkhusa VV, Condeelis J, Segall JE, van Rheezen J. Intravital imaging of metastatic behavior through a mammary imaging window. *Nat Meth* 5: 1019–1021, 2008.
53. Kerr JN, Denk W. Imaging in vivo: watching the brain in action. *Nat Rev Neurosci* 9: 195–205, 2008.
54. Kerschensteiner M, Schwab ME, Lichtman JW, Misdeld T. In vivo imaging of axonal degeneration and regeneration in the injured spinal cord. *Nat Med* 11: 572–577, 2005.
55. Kienast Y, von Baumgarten L, Fuhrmann M, Klunkert WE, Goldbrunner R, Herms J, Winkler F. Real-time imaging reveals the single steps of brain metastasis formation. *Nat Med* 16: 116–122, 2010.
56. Kiesslich R, Gossner L, Goetz M, Dahlmann A, Vieth M, Stolte M, Hoffman A, Jung M, Nafe B, Galle PR, Neurath MF. In vivo histology of Barrett's esophagus and associated neoplasia by confocal laser endomicroscopy. *Clin Gastroenterol Hepatol* 4: 979–987, 2006.
57. Kim JK, Choi JW, Yun SH. 350- μ m side-view optical probe for imaging the murine brain in vivo from the cortex to the hypothalamus. *J Biomed Optics* 18: 0505022979–050501, 2013.
58. Kim JK, Choi JW, Yun SH. Optical fine-needle imaging biopsy of the brain. *Biomed Optics Express* 4: 2846–2854, 2013.
59. Kim JK, Lee WM, Kim P, Choi M, Jung K, Kim S, Yun SH. Fabrication and operation of GRIN probes for in vivo fluorescence cellular imaging of internal organs in small animals. *Nat Protoc* 7: 1456–1469, 2012.
60. Kim JK, Vinarsky V, Wain J, Zhao R, Jung K, Choi J, Lam A, Pardo-Saganta A, Breton S, Rajagopal J. In vivo imaging of tracheal epithelial cells in mice during airway regeneration. *Am J Respir Cell Mol Biol* 47: 864, 2012.
61. Kim P, Chung E, Yamashita H, Hung KE, Mizoguchi A, Kucherlapati R, Fukumura D, Jain RK, Yun SH. In vivo wide-area cellular imaging by side-view endomicroscopy. *Nat Meth* 7: 303–305, 2010.
62. Kim TN, Goodwill PW, Chen Y, Conolly SM, Schaffer CB, Liepmann D, Wang RA. Line-scanning particle image velocimetry: an optical approach for quantifying a wide range of blood flow speeds in live animals. *PLoS One* 7: e38590, 2012.
63. Kreisel D, Nava RG, Li W, Zinselmeyer BH, Wang B, Lai J, Pless R, Gelman AE, Krupnick AS, Miller MJ. In vivo two-photon imaging reveals monocyte-dependent neutrophil extravasation during pulmonary inflammation. *Proc Natl Acad Sci USA* 107: 18073–18078, 2010.
64. Kreisel D, Sugimoto S, Zhu J, Nava R, Li W, Okazaki M, Yamamoto S, Ibrahim M, Huang HJ, Toth Ka Ritter JH, Krupnick AS, Miller MJ, Gelman AE. Emergency granulopoiesis promotes neutrophil-dendritic cell encounters that prevent mouse lung allograft acceptance. *Blood* 118: 6172–6182, 2011.
65. Laffray S, Pagès S, Dufour H, De Koninck P, De Koninck Y, Côté D. Adaptive movement compensation for in vivo imaging of fast cellular dynamics within a moving tissue. *PLoS One* 6: e19928, 2011.
66. Lee BT, Hutteman M, Gioux S, Stockdale A, Lin SJ, Ngo LH, Frangioni JV. The FLARE™ intraoperative near-infrared fluorescence imaging system: a first-in-human clinical trial in perforator flap breast reconstruction. *Plast Reconstr Surg* 126: 1472, 2010.
67. Lee JY, Park C, Cho YP, Lee E, Kim H, Kim P, Yun SH, Yoon Ys. Podoplanin-expressing cells derived from bone marrow play a crucial role in postnatal lymphatic neovascularization. *Circulation* 122: 1413–1425, 2010.
68. Lee S, Vinegoni C, Feruglio PF, Fexon L, Gorbato R, Pivoravov M, Sbarbati A, Nahrendorf M, Weissleder R. Real-time in vivo imaging of the beating mouse heart at microscopic resolution. *Nat Commun* 3: 1054, 2012.
69. Lee TR, Choi M, Kopacz AM, Yun SH, Liu WK, Decuzzi P. On the near-wall accumulation of injectable particles in the microcirculation: smaller is not better. *Sci Rep* 3: 2079, 2013.
70. Leunig M, Yuan F, Menger MD, Boucher Y, Goetz AE, Messmer K, Jain RK. Angiogenesis, microvascular architecture, microhemodynamics, and interstitial fluid pressure during early growth of human adenocarcinoma LS174T in SCID mice. *Cancer Res* 52: 6553–6560, 1992.
71. Li JL, Goh CC, Keeble JL, Qin JS, Roediger B, Jain R, Wang Y, Chew WK, Weninger W, Ng LG. Intravital multiphoton imaging of immune responses in the mouse ear skin. *Nat Prot* 7: 221–234, 2012.
72. Li W, Nava RG, Bribriescio AC, Zinselmeyer BH, Spahn JH, Gelman AE, Krupnick AS, Miller MJ, Kreisel D, Goldstein D. Intravital 2-photon imaging of leukocyte trafficking in beating heart. *J Clin Invest* 122: 2499–2508, 2012.
73. Llewellyn ME, Barretto RP, Delp SL, Schnitzer MJ. Minimally invasive high-speed imaging of sarcomere contractile dynamics in mice and humans. *Nature* 454: 784–788, 2008.
74. Llewellyn ME, Barretto RP, Delp SL, Schnitzer MJ. Minimally invasive high-speed imaging of sarcomere contractile dynamics in mice and humans. *Nature* 454: 784–788, 2008.
- 74a. Lok C. Imaging: cancer caught in the act. *Nature* 509: 148–149, 2014.
75. Looney MR, Thornton EE, Sen D, Lamm WJ, Glenn RW, Krummel MF. Stabilized imaging of immune surveillance in the mouse lung. *Nat Meth* 8: 91–96, 2011.
76. Mempel TR, Henrickson SE, von Andrian UH. T-cell priming by dendritic cells in lymph nodes occurs in three distinct phases. *Nature* 427: 154–159, 2004.
77. Miller MJ, Wei SH, Cahalan MD, Parker I. Autonomous T cell trafficking examined in vivo with intravital two-photon microscopy. *Proc Natl Acad Sci USA* 100: 2604–2609, 2003.
78. Misdeld T, Kerschensteiner M. In vivo imaging of the diseased nervous system. *Nat Rev Neurosci* 7: 449–463, 2006.
79. Monfared A, Blevins NH, Cheung EL, Jung JC, Popelka G, Schnitzer MJ. In vivo imaging of mammalian cochlear blood flow using fluorescence microendoscopy. *Otol Neurotol* 27: 144, 2006.
80. Mulligan SJ, MacVicar BA. Calcium transients in astrocyte endfeet cause cerebrovascular constrictions. *Nature* 431: 195–199, 2004.
81. Nishimura N, Schaffer CB, Friedman B, Tsai PS, Lyden PD, Kleinfeld D. Targeted insult to subsurface cortical blood vessels using ultrashort laser pulses: three models of stroke. *Nat Meth* 3: 99–108, 2006.
82. Novak J, Georgakoudi I, Wei X, Prossin A, Lin C. In vivo flow cytometer for real-time detection and quantification of circulating cells. *Optics Lett* 29: 77–79, 2004.
83. Nyman LR, Wells KS, Head WS, McCaughey M, Ford E, Brissova M, Piston DW, Powers AC. Real-time, multidimensional in vivo imaging used to investigate blood flow in mouse pancreatic islets. *J Clin Invest* 118: 3790, 2008.
84. Omenetto FG, Kaplan DL. A new route for silk. *Nat Photon* 2: 641–643, 2008.
85. Peti-Peterdi J, Toma I, Sipos A, Vargas SL. Multiphoton imaging of renal regulatory mechanisms. *Physiology* 24: 88–96, 2009.
86. Pittet MJ, Weissleder R. Intravital imaging. *Cell* 147: 983–991, 2011.
87. Presson RG, Brown MB, Fisher AJ, Sandoval RM, Dunn KW, Lorenz KS, Delp EJ, Salama P, Molitoris Ba, Pettrache I. Two-photon imaging within the murine thorax without respiratory and cardiac motion artifact. *Am J Pathol* 179: 75–82, 2011.
88. Ramiya VK, Maraist M, Arfors KE, Schatz DA, Peck AB, Cornelius JG. Reversal of insulin-dependent diabetes using islets generated in vitro from pancreatic stem cells. *Nat Med* 6: 278–282, 2000.
89. Ritsma L, Ellenbroek SI, Zomer A, Snippert HJ, de Sauvage FJ, Simons BD, Clevers H, van Rheezen J. Intestinal crypt homeostasis revealed at single-stem-cell level by in vivo live imaging. *Nature* 507: 362–365, 2014.
90. Ritsma L, Steller EJa Beerling E, Loomans CJM, Zomer A, Gerlach C, Vriskoop N, Seinstra D, van Gorp L, Schafer R, Raats Da, de Graaff a Schumacher TN, de Koning EJP, Rinkes IHB, Kranenburg O, Rheezen JV. Intravital microscopy through an abdominal imaging window reveals a pre-metastasis stage during liver metastasis. *Sci Trans Med* 4: 158ra145, 2012.
91. Ritsma L, Steller EJa Ellenbroek SIJ, Kranenburg O, Borel Rinkes IHM, Van Rheezen J. Surgical implantation of an abdominal imaging window for intravital microscopy. *Nat Prot* 8: 583–594, 2013.
92. Rompolas P, Deschene ER, Zito G, Gonzalez DG, Saotome I, Haberman AM, Greco V. Live imaging of stem cell and progeny behavior in physiological hair-follicle regeneration. *Nature* 487: 496–499, 2012.
93. Rompolas P, Mesa KR, Greco V. Spatial organization within a niche as a determinant of stem-cell fate. *Nature* 502: 513–518, 2013.
94. Rosivall L, Mirzahosseini S. Fluid flow in the juxtaglomerular interstitium visualized in vivo. *Am J Physiol Renal Physiol* 291: F1241–F1247, 2006.
95. Roussos ET, Balsamo M, Alford SK, Wyckoff JB, Gligorijevic B, Wang Y, Pozzuto M, Stobezki R, Goswami S, Segall JE, Lauffenburger Da Bresnick AR, Gertler FB, Condeelis JS. Mena invasive (MenaINV) promotes multicellular streaming motility and transendothelial migration in a mouse model of breast cancer. *J Cell Sci* 124: 2120–2131, 2011.
96. Russo LM, Sandoval RM, McKee M, Osicka TM, Collins aB, Brown D, Molitoris Ba, Comper WD. The normal kidney filters nephrotic levels of albumin retrieved by proximal tubule cells: retrieval is disrupted in nephrotic states. *Kidney Int* 71: 504–513, 2007.
97. Seeliger MW, Beck SC, Pereyra-Muñoz N, Dangel S, Tsai JY, Luhmann UF, van de Pavert SA, Wijnholds J, Samardzija M, Wenzel A. In vivo confocal imaging of the retina in animal models using scanning laser ophthalmoscopy. *Vision Res* 45: 3512–3519, 2005.
98. Sharma R, Yin L, Geng Y, Merigan WH, Palczewska G, Palczewski K, Williams DR, Hunter JJ. In vivo two-photon imaging of the mouse retina. *Biomed Optics Exp* 4: 1285–1293, 2013.
99. Shih AY, Blinder P, Tsai PS, Friedman B, Stanley G, Lyden PD, Kleinfeld D. The smallest stroke: occlusion of one penetrating vessel leads to infarction and a cognitive deficit. *Nat Neurosci* 16: 55–63, 2013.

101. Sipkins DA, Wei X, Wu JW, Runnels JM, Côté D, Means TK, Luster AD, Scadden DT, Lin CP. In vivo imaging of specialized bone marrow endothelial microdomains for tumour engraftment. *Nature* 435: 969–973, 2005.
102. Sokol H, Conway KL, Zhang M, Choi M, Morin B, Cao Z, Villablanca EJ, Li C, Wijmenga C, Yun SH. Card9 mediates intestinal epithelial cell restitution, T-helper 17 responses, and control of bacterial infection in mice. *Gastroenterology* 145: 591–601. e593, 2013.
103. Spencer JA, Ferraro F, Roussakis E, Klein A, Wu J, Runnels JM, Zaher W, Mortensen LJ, Alt C, Turcotte R. Direct measurement of local oxygen concentration in the bone marrow of live animals. *Nature* 508: 269–273, 2014.
104. Sumen C, Mempel TR, Mazo IB, von Andrian UH. Intravital microscopy: visualizing immunity in context. *Immunity* 21: 315–329, 2004.
105. Swirski FK, Nahrendorf M, Etzrodt M, Wildgruber M, Cortez-Retamozo V, Panizzi P, Figueiredo JL, Kohler RH, Chudnovskiy A, Waterman P. Identification of splenic reservoir monocytes and their deployment to inflammatory sites. *Science* 325: 612–616, 2009.
106. Tabuchi A, Mertens M, Kuppe H. Intravital microscopy of the murine pulmonary microcirculation. *J Appl Physiol* 104: 338–346, 2008.
107. Takano T, Tian GF, Peng W, Lou N, Libionka W, Han X, Nedergaard M. Astrocyte-mediated control of cerebral blood flow. *Nat Neurosci* 9: 260–267, 2006.
108. Truong TV, Supatto W, Koos DS, Choi JM, Fraser SE. Deep and fast live imaging with two-photon scanned light-sheet microscopy. *Nat Meth* 8: 757–760, 2011.
109. Verbeek FP, van der Vorst JR, Tummers QR, Boonstra MC, de Rooij KE, Löwik CW, Valentijn ARP, van de Velde CJ, Choi HS, Frangioni JV. Near-infrared fluorescence imaging of both colorectal cancer and ureters using a low-dose integrin targeted probe. *Ann Surg Oncol*. In press.
110. Vinegoni C, Lee S, Feruglio PF, Marzola P, Nahrendorf M, Weissleder R. Sequential average segmented microscopy for high signal-to-noise ratio motion-artifact-free in vivo heart imaging. *Biomed Opt Express* 4: 2095–2106, 2013.
111. Wang X, Arcuino G, Takano T, Lin J, Peng WG, Wan P, Li P, Xu Q, Liu QS, Goldman SA. P2X7 receptor inhibition improves recovery after spinal cord injury. *Nat Med* 10: 821–827, 2004.
112. Williams RM, Zipfel WR, Tinsley ML, Farnum CE. Solute transport in growth plate cartilage: in vitro and in vivo. *Biophys J* 93: 1039–1050, 2007.
113. Yanik MF, Cinar H, Cinar HN, Chisholm AD, Jin Y, Ben-Yakar A. Neurosurgery: functional regeneration after laser axotomy. *Nature* 432: 822, 2004.
114. Yeh AT, Nassif N, Zoumi A, Tromberg BJ. Selective corneal imaging using combined second-harmonic generation and two-photon excited fluorescence. *Optics Lett* 27: 2082–2084, 2002.
115. Yildiz A, Forkey JN, McKinney SA, Ha T, Goldman YE, Selvin PR. Myosin V walks hand-over-hand: single fluorophore imaging with 1.5-nm localization. *Science* 300: 2061–2065, 2003.
116. Yoo H, Kim JW, Shishkov M, Namati E, Morse T, Shubochkin R, McCarthy JR, Ntziachristos V, Bouma BE, Jaffer FA. Intra-arterial catheter for simultaneous microstructural and molecular imaging in vivo. *Nat Med* 17: 1680–1684, 2011.
117. Yuste R. Fluorescence microscopy today. *Nat Meth* 2: 902–904, 2005.
118. Zhong W, Celli J, Rizvi I, Mai Z, Spring B, Yun S, Hasan T. In vivo high-resolution fluorescence microendoscopy for ovarian cancer detection and treatment monitoring. *Br J Cancer* 101: 2015–2022, 2009.
119. Zipfel WR, Williams RM, Webb WW. Nonlinear magic: multiphoton microscopy in the biosciences. *Nat Biotechnol* 21: 1369–1377, 2003.
120. Ziv Y, Burns LD, Cocker ED, Hamel EO, Ghosh KK, Kitch LJ, El Gamal A, Schnitzer MJ. Long-term dynamics of CA1 hippocampal place codes. *Nat Neurosci* 16: 264–266, 2013.